Deducing *in Vivo* Toxicity of Combustion-Derived Nanoparticles from a Cell-Free Oxidative Potency Assay and Metabolic Activation of Organic Compounds

Tobias Stoeger, Shinji Takenaka, Birgit Frankenberger, Baerbel Ritter, Erwin Karg, Konrad Maier, Holger Schulz, and Otmar Schmid

Helmholtz Zentrum München, German Research Center for Environmental Health, Institute of Inhalation Biology, Neuherberg/Munich, Germany

Background: The inhalation of combustion-derived nanoparticles (CDNPs) is believed to cause an oxidative stress response, which in turn may lead to pulmonary or even systemic inflammation.

Objective and Methods: In this study we assessed whether the *in vivo* inflammatory response—which is generally referred to as particle toxicity—of mice to CDNPs can be predicted *in vitro* by a cell-free ascorbate test for the surface reactivity or, more precisely, oxidative potency (Ox_{Pot}) of particles.

Results: For six types of CDNPs with widely varying particle diameter (10–50 nm), organic content (OC; 1–20%), and specific Brunauer, Emmett, and Teller (BET) surface area (43–800 m^2/g), Ox_{Pot} correlated strongly with the *in vivo* inflammatory response (pulmonary polymorphonuclear neutrophil influx 24 hr after intratracheal particle instillation). However, for CDNPs with high organic content, Ox_{Pot} could not explain the observed inflammatory response, possibly due to shielding of the Ox_{Pot} of the carbon core of CDNPs by an organic coating. On the other hand, a pathway-specific gene expression screen indicated that, for particles rich in polycyclic aromatic hydrocarbon (PAHs), cytochrome P450 1A1 (CYP1A1) enzyme-mediated biotransformation of bioavailable organics may generate oxidative stress and thus enhance the *in vivo* inflammatory response.

Conclusion: The compensatory nature of both effects (shielding of carbon core and biotransformation of PAHs) results in a good correlation between inflammatory response and BET surface area for all CDNPs. Hence, the *in vivo* inflammatory response can either be predicted by BET surface area or by a simple quantitative model, based on *in vitro* Ox_{Pot} and *Cyp1a1* induction.

Key words: air pollution, BET, biotransformation, carbonaceous particles, *Cyp1a1*, dose response, nanoparticles, nanotoxicity, organic compounds, oxidative stress, particle toxicity, soot particles, specific surface area, surface toxicity, ultrafine particles. *Environ Health Perspect* 117:54–60 (2009). doi:10.1289/ehp.11370 available via *http://dx.doi.org/* [Online 22 August 2008]

Epidemiologic and clinical studies have linked elevated concentrations of ambient particulate matter (PM) to adverse health effects throughout the industrialized world (Kleeberger 2005). In urban environments, combustion-derived nanoparticles (CDNPs) such as soot particles dominate PM number concentrations and contribute significantly to the total PM surface area. Typically, these particles consist of a carbon core coated with potentially toxic air pollutants consisting of hundreds of organic chemicals and many transition metals (Kreyling et al. 2004; Oberdörster et al. 2005). At present, it is commonly hypothesized that the toxicity of ultrafine soot particles is largely driven by adsorbed redox-active components [e.g., polyaromatic hydrocarbons (PAHs)], which participate in redox-cycling reactions generating reactive oxygen species (ROS). These ROS can cause oxidative stress responses that may result in pulmonary or even systemic inflammation (Li et al. 2003a; Risom et al. 2005). Ultimately, these processes may promote the progression of atherosclerosis and precipitate acute cardiovascular responses ranging from increased blood pressure to myocardial infarction (Delfino et al. 2005). To counteract the adverse effects of oxidative stress generated by redox cycling and electrophilic compounds, nature "developed" an elaborate defense system to maintain redox homeostasis. This system includes a series of antioxidant enzymes, in particular, the so-called phase II xenobiotic metabolism enzymes that metabolize redox-cycling chemicals, eliminate excessive ROS, and protect cells against the damaging effects of electrophiles and oxidants (Winyard et al. 2005). A disturbance of the cellular redox equilibrium and related disproportionate oxidative stress is well known to trigger multiple stress kinase pathways and redox-sensitive transcription factors, such as nuclear factor-erythroid 2-p45–related factor 2 (Nrf2), which activates the expression of antioxidant and cytoprotective genes, as well as the nuclear localization of nuclear factor kappa B (NF-kB) and activator protein-1 (AP-1), which play key roles in gene promotion for inflammatory mediators (Cho et al. 2006; Rahman et al. 2006).

Identification of the particle properties that are most relevant for promoting adverse health effects is crucial not only for our mechanistic understanding but also for the implementation of strategies for improving air quality. For different kinds of particles with low toxicity and solubility, particle surface area has shown to be a useful dose metric for the characterization of particle-induced neutrophil response in the exposed lung (Oberdörster et al. 2005). Inflammatory effects of diesel exhaust particles (DEP) appear to be driven by particle surface area (Heinrich et al. 1995), although the type of organic (Baeza-Squiban et al. 1999) and metal (Ball et al. 2000) components also appear to play a role in oxidative and proinflammatory effects and subsequent pathogenicity. This is consistent with studies describing different classes of surface toxicity pointing to different pathways of particle-related stress induction (Dick et al. 2003; Donaldson et al. 2005; Duffin et al. 2002; Warheit et al. 2006).

In a previous study, we found that for six different types of CDNPs, the organic carbon content (OC) had a much weaker impact on the acute inflammatory response in the lungs of mice (24 hr after intratracheal instillation) than did Brunauer, Emmett, and Teller (BET) surface area, with predictive values of 0.0286 versus < 0.0001, respectively (Stoeger et al. 2006). Although BET surface area appears to be the single most relevant parameter for the prediction of particle toxicity, it is likely that other parameters such as the presence of free radicals, particle charge, and the bioavailability of adsorbed components may explain the observed differences in surface toxicity (Stoeger et al. 2006; Wittmaack 2007).

The objective of the present study was to assess the possibility of predicting particle toxicity based on the combined information from a cell-free *in vitro* test for the innate oxidative potency (Ox_{Pot}) of particles and a gene expression analysis targeting inflammation, stress, and detoxification-related genes. Here we relate the results from both tests to our

Address correspondence to T. Stoeger, Ingolstaedter Landstrasse 1, D-85758 Neuherberg/Munich, Germany. Telephone: 49-89-3187-3104. Fax: 49-89-3187-2400. E-mail: tobias.stoeger@helmholtz-muenchen.de

Supplemental Material is available online at http://www.ehponline.org/members/2008/11370/suppl.pdf

This work was funded by grant HL 70542 from the National Institutes of Health and by FE-76177 from the German National Genome Network.

The authors declare they have no competing financial interests.

Received 14 February 2008; accepted 22 August 2008.

previously published *in vivo* data on the acute inflammatory response of mice for six types of CDNPs (Stoeger et al. 2006) and introduce a simple two-parameter model to quantitatively describe the toxicity of CDNPs from the Ox_{Pot} and bioavailability of organic components. Ultimately, this model may serve as an additional step toward introducing a cell-free test for nanotoxicology that is reliable enough to make animal studies obsolete.

Materials and Methods

Particles. In the present study we used the same six CDNP types as we described previously (Stoeger et al. 2006). Briefly, we purchased DEPs [standard reference material SRM-1650a; National Institute of Standards and Technology (NIST), Gaithersburg, MD, USA] and PrintexG (PtxG) and Printex90 (Ptx90; pigment black; Degussa, Frankfurt, Germany) and generated and filter-sampled SootH (high OC), SootL (low OC), and ultrafine carbon particles (UfCPs) in our laboratory. We produced SootH and SootL particles by a well-controlled diffusion flame (CAST burner, Matter Engineering AG, Wohlen, Switzerland) with low and high oxygen-to-fuel ratios, respectively, resulting in soot particles with different amounts (and types) of organic compounds (Matuschek et al. 2007). The UfCPs, generated by spark discharge from graphite electrodes (GFG1000, Palas, Karlsruhe, Germany) (Roth et al. 2004), are noncombustion-derived particles with low OC, large specific surface area, and structural and compositional similarities with modern (Euro IV) diesel soot (Su et al. 2004). Table 1 lists the BET surface area [determined using the method described by Brunauer, Emmett, and Teller (1938)] and OC of all six particle types as reported previously (Stoeger et al. 2006) covering a wide range from about 40 to 800 m^2/g and from 1% to 20% OC. The (primary) particle diameter of the nanoparticle types ranged from about 10 to 50 nm (Stoeger et al. 2006). For the biological analysis of the CDNPs described below, we used the entire particles rather than solvent extracts.

Determination of the Ox_{Pot} of the particles. In living organisms, vitamin C (L-ascorbate), a highly effective antioxidant, is consumed as it protects the body against oxidative stress. Therefore, we used the depletion of ascorbate in an aqueous particle suspension as a cell-free *in vitro* test for the Ox_{Pot} of particles, where the absence of any metabolic activity in a cell-free system guarantees that this test characterizes the particles' innate (in absence of metabolic activation) Ox_{Pot} presumably related to the surface reactivity of the particles.

For each particle type, we incubated aliquots of 5, 1, and 0.2 µg for 40 min in an aqueous ascorbate solution (100 µL of 100 µM ascorbate in phosphate-buffered saline; this corresponds to 2.5 nmol ascorbate per 25 µL). After removal of the particles by centrifugation (30,000*g*/15 min/4°C), we quantified the antioxidative capacity of 25 µL of supernatant using the photochemiluminescence (PCL) method (Photochem, Analytik Jena AG, Jena, Germany), in which the fast photochemical excitation of radical formation is combined with sensitive luminometric detection (Popov and Lewin 1999). We performed two measurements for each particle type and concentration (Figure 1) and determined the particles' innate Ox_{Pot}, expressed as consumed ascorbate (nanomoles) per particle mass (micrograms) from the slope (not the ratio) of the measured ascorbate consumption and particle mass in order to avoid biases due to potential zero offsets. For UfCP and SootL particles, the highest dose of 5 µg had to be discarded because a consumption of 2.4 nmol of 2.5 nmol ascorbate points to saturation issues.

Determination of the inflammatory efficacy of the particles. In the present study, we used the *in vivo* animal exposure data from our previous study (Stoeger et al. 2006). In brief, for each particle type, we determined the response of eight female BALB/cJ mice (21.1 ± 1 g) after intratracheal instillation of 5, 20, or 50 µg CDNPs in 50 µL aqueous suspension or pure water (sham control), except for UfCP, which also included instillations with 0.5 and 2 µg particles. We treated animals humanely and with regard for alleviation of suffering; experimental protocols were reviewed and approved by the Bavarian Animal Research Authority (approval no. 211-2531-108/99). At 24 hr after instillation, we performed bronchoalveolar lavage (BAL) and assessed BAL fluid for polymorphonuclear neutrophils (PMNs) as a measure of the inflammatory cellular response. In the present study, the previously reported absolute numbers of PMNs (Stoeger et al. 2006) were normalized by the number of BAL leukocytes [Supplemental Material, Figure 1 (http://www.ehponline.org/members/2008/11370/suppl.pdf)], thus eliminating some bias due to varying effectiveness of cell retrieval by the lavage procedure (especially for 50 µg PtxG).

Using these data, in the present study we defined the (*in vivo*) inflammatory efficacy (I_{Ef}) as the 20% PMN effect level divided by the particle mass causing this effect level ($M_{20\%PMN}$), that is, I_{Ef} = 20% PMN/$M_{20\%PMN}$ (%PMN/µg). We chose the 20% PMN threshold because it is significantly different from the sham response (~ 2%), it is clearly beneath saturation levels (> 40%), and it is exceeded by all six particle types [See Supplemental Material, Figure 1 (http://www.ehponline.org/members/2008/11370/suppl.pdf)]. We derived the $M_{20\%PMN}$ values by interpolation between the two PMN data points bracketing the 20% effect level.

Quantification of gene and protein expression. For expression analysis, lavaged lungs from the 20 µg exposure were homogenized using the FastPrep FP120 Cell Disruptor (BIO101/Savant Instruments Inc., Holbrook, NY, USA) automat with Lysing Matrix Tube D (MP Biomedicals, Illkirch, France) and subjected to either RNA or protein extraction (four mice per group). RNA isolation from lung homogenates was processed using the RNeasy Kit (Qiagen, Hilden, Germany). For quantitative reverse-transcriptase polymerase chain reaction (PCR), we used

Table 1. Physicochemical and biological particle properties.

Particle	BET surface area (m^2/g)	Percent OC (NIOSH 5040)[a]	I_{Ef} (% PMN/µg)	Ox_{Pot} (nmol/µg)[b]	R^{2c}
UfCP	800	17 (< 5)[d]	4.8	0.839	1.00[e]
SootL	441	7	2.5	0.617	1.00[e]
SootH	268	19	1.7	0.057	0.99
Ptx90	272	2	1.2	0.278	1.00
DEP	108	20[f]	0.5	0.026	0.27[g]
PtxG	43	1	0.4	0.024	0.88

[a]The organic carbon fraction was determined with a thermooptical method according to the National Institute for Occupational Safety and Health (NIOSH) 5040 standard protocol (Cassinelli and O'Connor 1998). [b]Ox_{Pot} from the slope of the consumed ascorbate versus particle mass (see Figure 1). [c]R^2 gives the significance (goodness of fit) of the linear regression. [d]The NIOSH 5040 value of 17% (Stoeger et al. 2006) is unrealistically high for spark-generated (pure) carbon particles; more detailed chemical analysis suggests that UfCPs contained < 5% of organic matter (Frampton et al. 2004; Matuschek et al. 2007). [e]Here R^2 = 1 because only two data points were available for UfCP and SootL because of saturation issues (see Figure 1). [f]This value was not obtained according to the NIOSH protocol; it refers to the solvent (Soxhlet)-extractable mass fraction as reported by NIST (2000). [g]The low R^2 value is at least in part due to the small effect level for DEP.

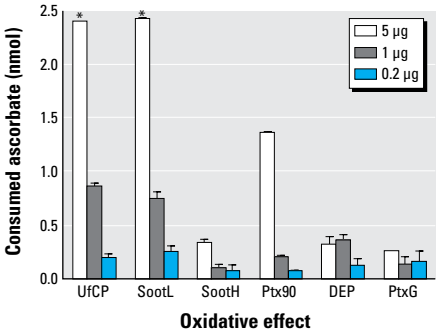

Figure 1. Cell-free oxidative effect (mean ± SE) of the six types of CDNP displayed as the amount of ascorbate consumed by the respective particle mass (5, 1, and 0.2 µg).

*Values that were negatively biased because of their proximity to the saturation level (2.5 nmol) were discarded for the calculation of Ox_{Pot} (Table 1).

1 µg total DNase I–treated RNA for the first-strand cDNA reaction using hexamer primer (Promega, Mannheim, Germany) and Superscript II reverse transcriptase (Invitrogen, Karlsruhe, Germany). We pooled cDNA samples from each experimental group and quantified transcript levels using Absolute QPCR SYBR Green Mix plus ROX kit (ABgene, Hamburg, Germany) with the ABI Prism 7000 Sequence Detection System (Applied Biosystems, Foster City, CA, USA). We used the comparative C_T (threshold cycle) method to calculate the relative abundance of transcript (Applied Biosystems 1997). For normalization, we used 18S RNA [GenBank accession no. NT_039649.7 (National Center for Biotechnology Information 2008)] as the reference gene to derive the fold increase in relation to the sham control group. Details of the primer and sequence specifications are given in Supplemental Material, Table 1 (http://www.ehponline.org/members/2008/11370/suppl.pdf).

We performed extraction of cytoplasmic lung protein in RIPA buffer plus Protease Inhibitor Cocktail III (Merck Chemicals, Darmstadt, Germany). We pooled 20 µg of total lung protein from each of the eight experimental groups (six CDNP types and two controls) and separated it by sodium dodecyl sulfate gel electrophoresis using the XCell II Blot Module and NuPage Novex Bis-Tris Gels and blotted to polyvinyl difluoride membranes (Invitrogen). The following primary antibodies were used: rabbit anti-cyclooxygenase-2 (COX2; ab15191; Abcam, Cambridge, UK), rabbit anti-cytochrome P450 1A1 (CYP1A1; sc-20772; Santa Cruz Biotechnology, Heidelberg, Germany), rabbit anti-rat liver glutathione *S*-transferase α1 (GST-Ya; AB 0009; Gentaur, Aachen, Germany), rabbit anti-heme oxygenase-1 (HO1; SPA 895; Biomol, Hamburg, Germany), rabbit anti-heat shock 70-kDa protein 1B (HSP70; SPA 812, Biomol), goat anti-NAD(P)H dehydrogenase [quinone] 1 (NQO1; IMG-3033, Biomol), and, as loading control, mouse monoclonal anti–β-actin (ACTB), AC-15 (A1978; Sigma-Aldrich, Taufkirchen, Germany). We applied horseradish peroxidase–linked species-specific secondary antibody for primary antibody detection, donkey anti-rabbit IgG (Amersham/GE Healthcare, Buckinghamshire, UK), rabbit anti-goat (Chemicon International, Millipore Corp., Billerica, MA, USA), and sheep anti-mouse (Amersham/GE Healthcare), using the ECT Plus Detection System (Amersham/GE Healthcare). Scanned blots were analyzed using the Syngene software image analysis program (Syngene, Cambridge, UK) with baseline correction setting "rolling disc." Protein expression derived from quantified densities of respective bands were normalized to ACTB and expressed as fold change relative to sham controls.

Statistical analyses. All values are reported as the mean ± SE. We used analysis of variance calculated by Statgraphics software (STSC Inc., Rockville, MD, USA) to establish the statistical significance of differences between the experimental groups. We applied the Tukey honestly significant difference procedure to evaluate the significant differences between the exposed animals and the sham control group. We considered differences significant at $p < 0.05$.

Results

In vitro* Ox_{Pot}, *in vivo* I_{Ef}, *and surface area of the particles. As indicated in our previous study (Stoeger et al. 2006), Figure 2A confirms the excellent linear correlation between inflammatory response and BET surface area for the six types of CDNPs used in the present study. For a wide dynamic range of more than a factor of 10 (with UfCP and PtxG at the upper and lower end, respectively), the differences in BET surface area explain 98% (R^2) of the observed variability in I_{Ef}. Neglecting the small intercept of 0.055% PMN/µg, the slope of 0.006% PMN/mm^2 indicates that, on average, a particle surface area of 33 cm^2 is required to induce a 20% influx of PMNs into the lungs. Figure 2B shows a reduced but still strong linear correlation between the I_{Ef} and Ox_{Pot} of the particles (R^2 = 0.77; $I_{Ef} = 5.14 Ox_{Pot}$; forced through the origin) with an identical order of descending I_{Ef} and Ox_{Pot} except for SootH, which has a more than three times higher I_{Ef} than expected from its Ox_{Pot}. This can be interpreted as a reduced surface-specific Ox_{Pot}, as illustrated in Figure 2C, which clearly shows SootH (and, to a lesser degree, DEP) below the trend line based on the other four data points.

Gene expression analysis reveals bioactivation of particle-borne organics. To identify the reason for the irregular behavior of SootH, in the lungs of mice 24 hr after the instillation of 20 µg of SootH, we analyzed the expression patterns of 50 genes representing different biologic response types, including inflammation, stress response, metal detoxification, and phase I and II detoxification of xenobiotics such as PAHs.

Table 2 displays the expression of the 22 most notably regulated genes [see also Supplemental Material, Figure 2 (http://www.ehponline.org/members/2008/11370/suppl.pdf)] in terms of fold induction in relation to sham controls; that is, unity represents the absence of gene regulation. We averaged the abundances of proinflammatory marker genes (rows 2 through 9) in Table 2 for each particle type to obtain a mean score for a transcriptional proinflammatory response—"proinflammatory synopsis." Ranking the particles in terms of the proinflammatory synopsis (Table 2) and PMN-based cellular lung inflammation (I_{Ef} in Table 1) shows good agreement and validates the relevance of our RNA expression data.

We gained insight into transcriptional regulations related to general stress response by examining the inducible 70-kDa heat shock gene *Hsp1a1* as well as the metallothionein 1 and 2 genes (*Mt1* and *Mt2*), all known to be up-regulated directly by oxidative stress and toxic chemicals—particularly heavy metals. Only PtxG particles showed a more than 2-fold increase in *Hsp1a1* lung transcript levels 24 hr after instillation; for the other carbon black sample (Ptx90), mRNA levels were 3-fold decreased. Gene expression of *Mt1* and *Mt2* was increased for UfCP only; for DEP, these genes were 2-fold repressed. This indicates that, although the toxicity of metals may have contributed to the oxidative stress

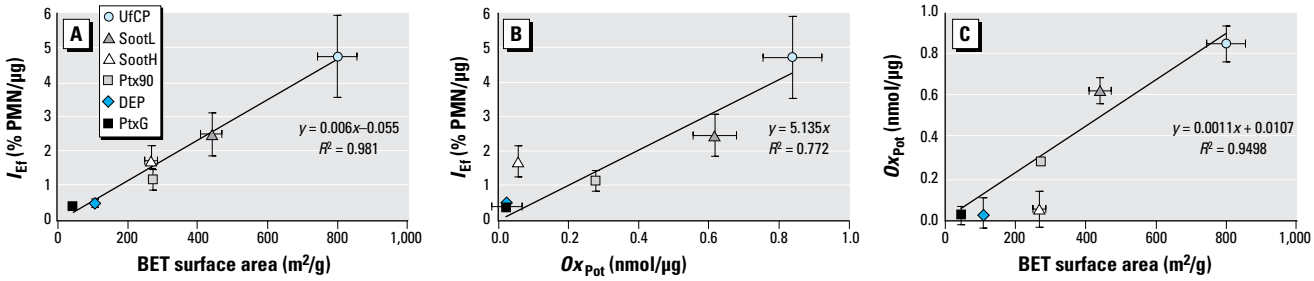

Figure 2. Relationships between the *in vitro* Ox_{Pot}, *in vivo* I_{Ef}, and BET surface area of the six types of CDNPs. (*A*) BET surface area versus I_{Ef} with the linear regression line. (*B*) Ox_{Pot} versus I_{Ef} (the linear regression line was forced through the origin). (*C*) BET surface area versus oxidative potency (the linear regression was based on all data points except SootH and DEP).

induced by UfCP and DEP, metals do not explain the extreme deviation of SootH from the linear response curve or the general trend in Figure 2B.

The expression analysis of 11 selected detoxification enzymes (*Cyp1a1*, *Cyp1b1*, *Aldh3a1*, *Gclc*, *Gpx1*, *Gpx4*, *Gsr*, *Gsta1*, *Hmox1*, *Nqo1*, and *Ogg1*) revealed that each particle type induced at least one of these genes. However, the only gene whose expression was induced specifically by SootH (3.9-fold up-regulated) and, to a lower extent, by DEP (1.6-fold up-regulated) was the phase I xenobiotic metabolizing enzyme *Cyp1a1*. To validate these data derived from pooled samples, we also quantified *Cyp1a1* expression in SootH-instilled mice on the single-animal level (n = 4). Single-animal analysis confirmed our previous data detecting an induction of 4.0 ± 0.4 that is significantly (p = 0.001) different from sham controls [see Supplemental Material, Figure 2 (http://www.ehponline.org/members/2008/11370/suppl.pdf)]. Furthermore, low-OC particles (OC < 7%) were either not significantly affected (Ptx90, PtxG) or down-regulated (SootL, UfCP). In contrast to *Cyp1a1*, the closely related cytochrome 450 phase I enzyme isoform *Cyp1b1* did not show regulation by more than 2-fold. The investigated phase II enzymes *Gclc*, *Gpx1*, *Gpx4*, and *Gsr* were more than 2-fold induced by UfCP, but none of them was more than 2-fold induced by the OC-rich DEP and SootH particles. 8-Oxoguanine DNA glycosylase (Ogg1), a DNA repair enzyme whose expression is associated with organics-related DNA adduct formation (Sorensen et al. 2003), is more than 2-fold induced by Ptx90 and UfCP and thus also is not a suitable marker for OC-rich particle instillation.

In summary, our expression data identify *Cyp1a1* as the only marker gene whose expression is specifically induced by OC-rich particle exposure.

OC-rich soot particles induce expression of CYP1A1 protein in the lung. Because the functional relevance of induced gene expression needs to be confirmed by a subsequent increase in expressed protein levels, we analyzed six of the investigated marker genes (*Hmox1*, *Ptgs2*, *Cyp1a1*, *Gsta1*, *Hsp1a1*, and *Nqo1*) on the protein level (HO1, COX2, CYP1A1, GSTYa1, HSP70, and NQO1) by immunoblotting of cytoplasmic extracts from lungs 24 hr after particle instillation (Figure 3). As expected from our mRNA data, only the expression of CYP1A1 protein was strongly induced by instillation of OC-rich SootH particles. Moreover, particle exposure did not influence the abundance of any of the other investigated proteins. Quantification of protein expressions relative to sham control and normalized to ACTB revealed a 21-fold induction of CYP1A1 protein expression for SootH particles and a 1.6- and 1.4-fold induction for DEP and PtxG, respectively. UfCP and Ptx90 particle instillation suppressed expression of the CYP1A1 protein to 40% and 30% of control levels, respectively. CYP1B1 was not detectable at all (not shown in Figure 3), and the phase II enzymes NQO1, GSTYa1, and HO1 did not indicate specific responses at the 24-hr time point. The inflammatory mediator COX2 (*Ptgs2*) was suppressed up to 2-fold 24 hr after instillation of all particles.

Immunohistologic localization of CYP1A expression. Immunohistologic detection of CYP1A1 protein expression in lungs 24 hr after instillation of 20 µg particles revealed the strongest expression for SootH-exposed lungs (Figure 4) and somewhat weaker signals for DEP-exposed lungs (data not shown). We identified CYP1A1-positive cells to be mainly alveolar epithelial cells, but we also identified some positive alveolar macrophages. No clear signal could be detected in lungs from untreated and sham-exposed mice or after UfCP, Printex, or SootL instillation.

Discussion

Ox_{Pot} is a strong indicator for particle-induced inflammatory effects. Several studies indicate that the Ox_{Pot} of the particle surface is critical for biologic responses related to

Table 2. Gene expression analysis (fold change relative to sham control) showing the mean transcript abundance assessed by quantitative PCR in the lungs of mice 24 hr after instillation of six types of CDNPs (20 µg).

Pathway	Gene	DEP	PtxG	Ptx90	SootH	SootL	UfCP
Proinflammatory	*Csf2*	2.0	2.0	5.2	5.7	6.5	3.4
	Cxcl1	0.7	1.9	4.0	5.6	7.5	15.9
	Cxcl5	0.4	2.5	2.4	4.9	4.4	9.6
	Il6	1.0	1.5	1.7	3.0	5.5	5.6
	Il1b	0.9	1.1	1.7	1.8	1.8	1.0
	Mmp9	0.8	1.6	1.9	2.4	1.7	2.6
	Ptgs2	1.1	2.1	1.4	1.4	1.3	1.1
	Tnfa	1.3	0.9	1.6	1.8	2.1	0.9
Proinflammatory synopsis		1.0	1.7	2.5	3.3	3.9	5.0
Stress response	*Hspa1a*	0.6	2.6	0.3	0.7	1.0	1.5
	Mt1	0.5	1.6	0.9	1.4	1.1	4.4
	Mt2	0.4	0.8	1.1	1.1	1.3	3.6
Detoxification, phase I	*Cyp1a1*	1.6	1.2	0.9	3.9	0.4	0.4
	Cyp1b1	0.6	0.7	0.8	1.4	1.3	0.7
Detoxification, phase II	*Aldh3a1*	0.4	0.5	0.6	1.0	0.6	0.5
	Gclc	0.8	2.4	1.5	1.5	1.9	4.3
	Gpx1	0.9	1.4	1.2	1.3	1.3	3.1
	Gpx4	0.6	0.8	0.9	0.8	0.8	3.1
	Gsr	0.7	2.1	1.3	1.2	1.3	2.5
	Gsta1	0.5	0.5	0.6	1.0	0.7	0.5
	Hmox1	1.1	1.8	1.6	1.9	1.9	0.9
	Nqo1	1.1	2.2	2.0	1.9	1.7	0.9
	Ogg1	1.3	1.9	2.8	1.9	1.5	2.5

We examined 50 genes related to various cellular response pathways, with the 22 most notably changed included here. Averaging expression levels for the eight genes indicative for the inflammatory pathway (proinflammatory synopsis) provides a proxy for the severity of inflammation.

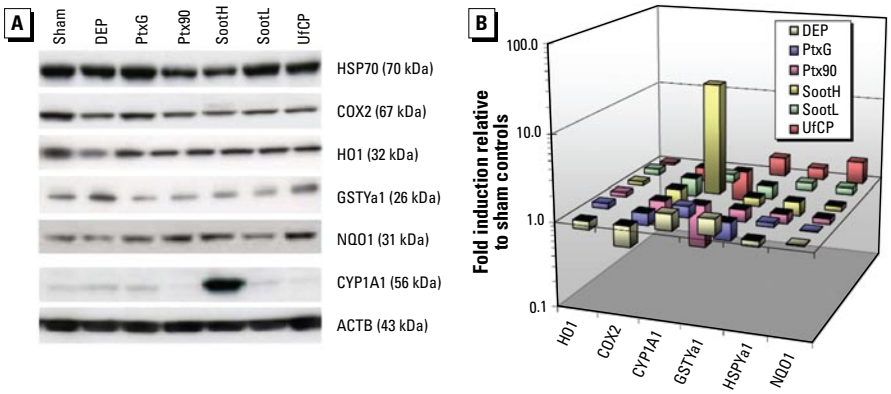

Figure 3. Protein expression and quantification of selected markers. (*A*) Protein expression analyzed by immunoblotting. (*B*) For quantification, signal densities were normalized to ACTB loading control and are displayed relative to the respective expressions in sham controls. CYP1A1 was the only marker that was induced for the known high-OC particles SootH (21-fold) and DEP (1.6-fold). It even was mildly induced for PtxG (1.4-fold).

inflammation (Beck-Speier et al. 2005; Li et al. 2003b; Xia et al. 2006). Because for the six types of CDNPs investigated here the Ox_{Pot} (based on a cell-free assay) can explain only about 80% of the observed variability in I_{Ef} (R^2 = 0.77; Figure 2B), at least one more parameter contributes to the observed *in vivo* particle toxicity (I_{Ef}). Furthermore, particles with high OC (DEP, SootH) display a mitigated surface-specific Ox_{Pot} compared with low-OC particles (Figure 2C). This could indicate that an organic coating shields the active structures at the surface of the carbon matrix and thus prevents radical formation. On the other hand, if Ox_{Pot} were the only pathway of inflammation, the surface-specific I_{Ef} of DEP and SootH should be reduced compared with low-OC particles (e.g., SootL, UfCP). Because Figure 2A does not show this (DEP and SootH do not lie significantly below the linear regression curve), the mitigating effect of the organic coating on Ox_{Pot} is compensated by another mechanism, which only occurs in the *in vivo* and not in the *in vitro* test.

Biotransformation of particle-adsorbed organics contributes to inflammatory effects. The prime candidates for this additional mechanism are the enzymatic biotransformation of initially nontoxic (nonoxidizing) organic compounds into toxic derivatives and, to a lesser degree, the nonenzymatic, catalyst-mediated formation of free radicals such as hydroxyl radicals via Fenton chemistry by, for example, transition metals. The latter would not necessarily require a metabolic active cell, and the corresponding Ox_{Pot} would probably be detected by our ascorbate-PCL–based Ox_{Pot} measurement. However, the fact that metal-inducible *Mt1* and *Mt2* genes (Adams et al. 2002) were not up-regulated by DEP and SootH (Table 2) suggests no metal involvement.

On the other hand, the induced expression of both the *Cyp1a1* gene and CYP1A1 protein for SootH (3.9- and 21-fold for gene and protein, respectively) and, to a much lesser degree, for DEP (1.6-fold for both gene and protein) indicates that metabolic detoxification of organics takes place for particles with high OC. In addition, PtxG, the particle type with the lowest OC (1%), also shows a small induction (1.2- and 1.4-fold for gene and protein, respectively). All other low-OC particles show a down-regulation in both the *Cyp1a1* gene and CYP1A1 protein. Hence, it is obviously not only the amount of organics, but also the type of organics, that determines the regulation of *Cyp1a1*.

Pulmonary expression of *Cyp1a1* has previously been identified as a possible biomarker of exposure to DEPs *in vitro* and *in vivo* (Bonvallot et al. 2001; Takano et al. 2002). For instance, Takano et al. (2002) instilled DEP from a light-duty automobile source and observed *Cyp1a1* transcript levels to be about 5-fold induced 24 hr after instillation of 50 µg DEP per mouse, whereas no effect was detected for 10 µg. (Bonvallot et al. 2001, Takano et al. 2002). This is consistent with results from our present study, in which instillation of 20 µg DEP from a heavy-duty diesel engine (SRM 1650a) mildly induced the *Cyp1a1* expression on RNA and protein level (1.6-fold).

Two main families of organic compounds that are known to be adsorbed onto ambient CDNPs are PAHs and quinones (Health Effects Institute 2002). After cellular uptake, PAHs could be desorbed from the CDNPs, become bioavailable to bind to the cytosolic aryl hydrocarbon receptor (AHR) and thereby induce target gene expression such as that of phase I metabolizing cytochrome P450 enzymes. The toxicity of many PAHs is known to depend on their bioactivation by P450 enzymes (Ramadoss et al. 2005). The hypothesis of PAH-related bioactivation of toxic compounds for SootH and DEP (as well as for PtxG) is supported by the chemical analysis of the particles. Both liquid chromatography and thermoanalytical investigation have revealed significant amounts of PAHs for SootH (~ 1%), exceeding those from SootL by a factor of about 50 (Schroeppel et al. 2003). Moreover, detailed chemical speciation reveals the presence of aromatic compounds such as benz(*a*)anthracene, benzo(*k*) fluoranthene, and/or benzo(*a*)pyrene, in significant amounts only on SootH, DEP, and PtxG samples (Matuschek et al. 2007; NIST 2000), which have been described as potent inducers of *Cyp1a1* (Till et al. 1999).

Mechanistic considerations. PAH metabolism by *Cyp1a1* produces reactive electrophilic metabolites, including ROS (Baulig et al. 2003; Martignoni et al. 2006). In the present study, we did not directly quantify ROS formation in the lungs of instilled mice, but we quantified several proinflammatory genes that are known to be regulated by redox-sensitive transcription factors such as NF-kB and AP-1 (Cho et al. 2006; Rahman et al. 2006). *In vivo* we found the lung transcripts for the cytokines *Csf2*, *Cxcl1*, *Cxcl5*, and *Il6*—all known to be largely regulated by NF-kB and AP-1 (reviewed by Castranova 2004)—to be induced by SootH and SootL instillation at a similar level (Table 2), whereas the *in vitro* Ox_{Pot} of SootL exceeded that of SootH by a factor of about 6 (Figure 2B). Again, this suggests that two different mechanisms are responsible for the toxicity of SootL and SootH particles, one related to the particles' innate Ox_{Pot} and the other possibly to bioactivation of organics.

Interestingly, compared with sham controls, mice instilled with SootL and UfCP had *Cyp1a1* expression that was about 3-fold down-regulated; these are the two particle types with the highest innate Ox_{Pot}, and the very same particles caused the strongest expression of the proinflammatory mediators (*Cxcl1*, *Cxcl5*, and *Il6*), which are regulated by redox-sensitive transcription factors. Hence, the transcriptional repression of *Cyp1a1* might be explained by

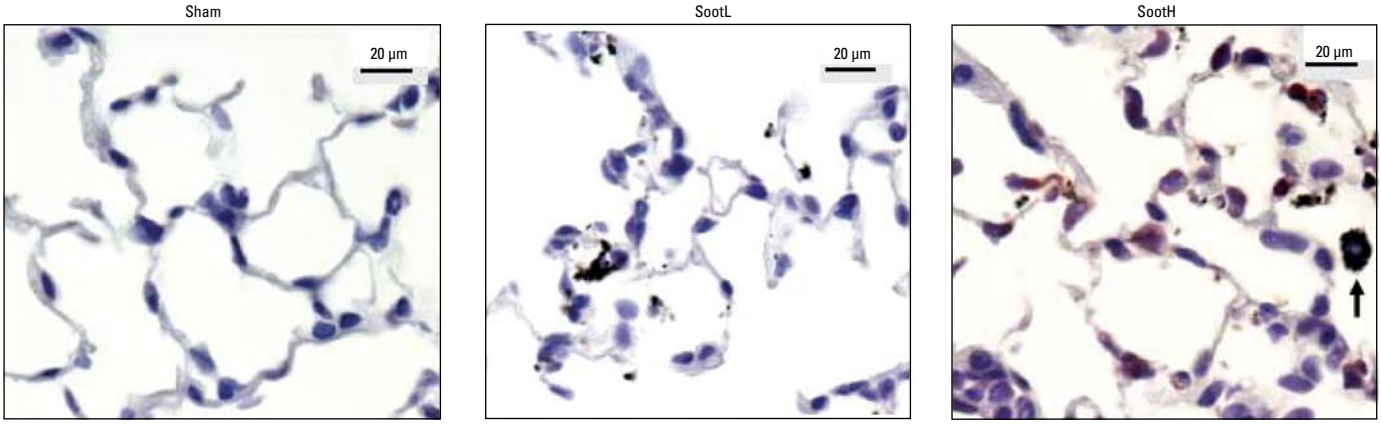

Figure 4. Immunohistologic staining of CYP1A1 protein expression in lungs 24 hr after 20 µg particle instillation showed broad positive staining in epithelial cells (red) and some alveolar macrophages (data not shown) of SootH-exposed mice. No staining was detected in sham- or SootL-exposed lungs. Agglomerates from SootH and SootL particles are clearly visible in the lungs. The arrow indicates a SootH-loaded macrophage containing agglomerated particles.

inhibition of *Cyp1a1* RNA expression by oxidative stress in general. This interpretation is consistent with the autoregulatory mechanism described by Morel et al. (1999) in a human hepatoma cell line; they found that intracellular ROS production disturbs the AHR-dependent induction of *Cyp1a1* expression, which represents a protective negative feedback loop. Alternatively, Gharavi and El-Kadi (2005) showed in murine hepatoma cell lines that *Cyp1a1* is down-regulated by the proinflammatory cytokines interleukin 1β (Il-1β), IL-6, and tumor necrosis factor α in an AHR-dependent manner. Even though both models address the liver and not the lung as studied here, this autoregulatory, ROS-protective mechanism could explain our observation that CDNPs with high innate Ox_{Pot} induce significant down-regulation of *Cyp1a1* expression.

Cyp1a1 and *Cyp1b1*, two closely related and essential extrahepatic phase I P450 monooxygenases, are highly inducible in the human lung by certain aromatic compounds, such as benzo(*a*)pyrene, via AHR signaling (reviewed by Martignoni et al. 2006). However, with our instillation approach we observed no dependence of *Cyp1b1* mRNA expression on organic compounds, because expression levels relative to controls were weakly induced by SootH to an expression level that is identical to that of SootL (1.4-fold). This apparent contradiction to the high expression of *Cyp1a1* by SootH can be resolved if one considers that despite their close functional relationship, the CYP1A1 and CYP1B1 isoforms are regulated in a different manner. For example, *Cyp1a1* transcript expression is repressed by proinflammatory cytokines (Gharavi and El-Kadi 2005), whereas *Cyp1b1* expression is induced (Piscaglia et al. 1999). In this context, cAMP response elements as well as AP-1 sites—both frequently involved in proinflammatory signaling—have been identified in the murine *Cyp1b1* but not *Cyp1a1* promoter (Zheng and Jefcoate 2005).

In summary, our results support the following mechanistic scheme (Figure 5) for particle-related inflammation: On the one hand, particles with high innate Ox_{Pot} (linked to low OC) generate direct oxidative stress by particle–cell interaction, which in turn activates redox-sensitive transcription of proinflammatory genes (pathway 1). On the other hand, particles with high amounts of bioavailable OC, such as PAHs, first induce phase I detoxification enzymes—in particular, CYP1A1 in exposed cells (pathway 2). Increased activity of CYP1A1 monooxygenase in turn leads to biotransformation and bioactivation of PAHs with associated ROS formation. Consequently, the induced oxidative stress activates transcription of both proinflammatory and phase II detoxification genes. The latter facilitate metabolization and conjugation of the highly active transformed organic compounds, ultimately leading to their elimination from the organism (Köhle and Bock 2007).

***Quantitative model for* I_{Ef}.** The analysis presented here can be used to derive a simple, quantitative model for predicting the *in vivo* toxicity of CDNPs based on a simple *in vitro* assay for Ox_{Pot} and (*in vivo*) *Cyp1a1* gene or protein expression. As a first approach, we performed a linear regression (forced through the origin) with the ascorbate-based *in vitro* test (Ox_{Pot}) as independent and I_{Ef} as dependent parameters to obtain

$$I_{Ef} = 5.14 Ox_{Pot} \text{ (nmol/µg)}. \quad [1]$$

As a second approach, we modeled the *in vivo* I_{Ef} as linear function of both Ox_{Pot} and *Cyp1a1* gene expression (GE_{Cyp1a1} expressed as fold induction after instillation of 20 µg particles), yielding

$$I_{Ef} = 5.14 Ox_{Pot} \text{ (nmol/µg)} + 0.509(GE_{Cyp1a1} - 1), \quad [2]$$

where we set GE_{Cyp1a1} to unity (no contribution from pathway 2), if *Cyp1a1* was down-regulated (< 1-fold). As shown in Figure 6A, the one-parameter model (pathway 1 only; Equation explains only 77% of the observed variability in I_{Ef}, whereas the two-parameter model, which considers contributions from pathways 1 and 2 (Equation 2), explains 94%. This indicates that both pathways contribute to the observed I_{Ef}. Because the small data set (six data points) required limiting the number of independent fit parameters, we reduced the number of fit parameters to two

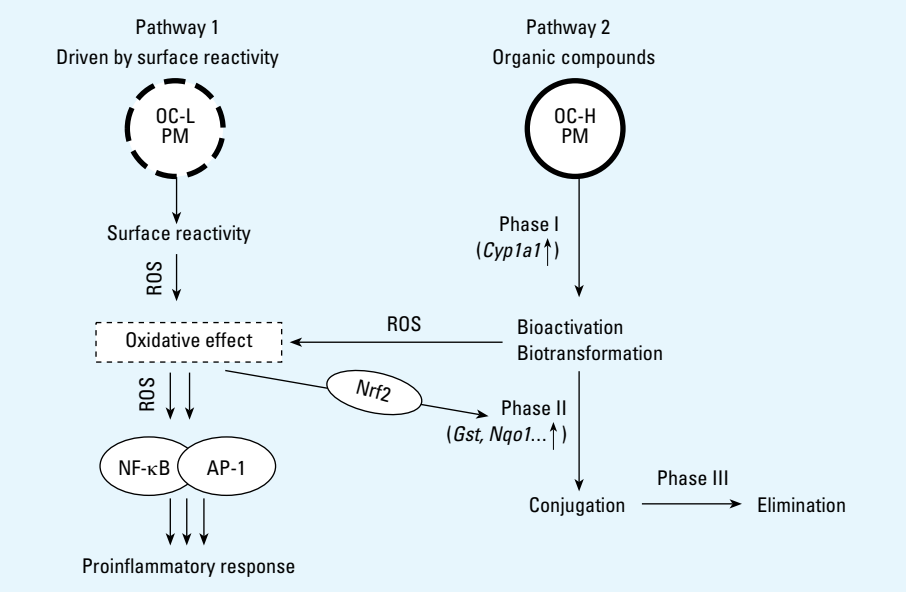

Figure 5. Mechanistic model for particle-related proinflammatory response that is consistent with our *in vivo* and *in vitro* data for CDNPs. The inflammatory signaling cascade is activated by oxidative stress due to the combined effects of the particles' innate surface reactivity (measured as Ox_{Pot}; pathway 1) and the presence of bioavailable organic compounds (*Cyp1a1* induction; pathway 2), which are eliminated via a three-phase detoxification process. Abbreviations: H, high; L, low; PM, particulate matter.

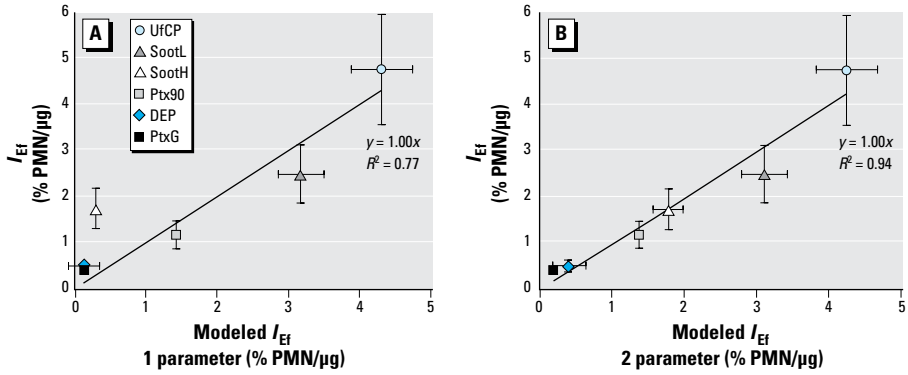

Figure 6. The predictive capacity of two simple linear models for the measured I_{Ef}. Although the one-parameter regression model based on Ox_{Pot} only ($I_{Ef} = 5.14 Ox_{Pot}$) represents 77% of the observed variability in I_{Ef}, the two-parameter model (Ox_{Pot} and *Cyp1a1* induction; see Equation 2), which considers the combined effects of pathway 1 and pathway 2, explains about 94%.

by assuming linearity (through the origin) and independence of pathways 1 and 2 (see Equation 2). Although this is likely to be only a crude approximation for complex biological systems, the agreement between measured and modeled I_{Ef} is remarkable.

Because we derived our expression data from *in vivo* experiments, this model for toxicity prediction still requires animal exposures, although at a reduced amount. However, if future research will provide a means of obtaining *Cyp1a1* expression data from the exposure of cell lines, the nanotoxicologic model we present here may provide a true alternative to animal exposures.

References

Adams TK, Saydam N, Steiner F, Schaffner W, Freedman JH. 2002. Activation of gene expression by metal-responsive signal transduction pathways. Environ Health Perspect 110(suppl 5):813–817.

Applied Biosystems. 2001. Relative Quantitation of Gene Expression. ABI PRISM 7700 Sequence Detection System: User Bulletin 2. Available: http://www3.appliedbiosystems.com/cms/groups/mcb_support/documents/generaldocuments/cms_040980.pdf [accessed 3 December 2008].

Baeza-Squiban A, Bonvallot V, Boland S, Marano F. 1999. Airborne particles evoke an inflammatory response in human airway epithelium. Activation of transcription factors. Cell Biol Toxicol 15:375–380.

Ball JC, Straccia AM, Young WC, Aust AE. 2000. The formation of reactive oxygen species catalyzed by neutral, aqueous extracts of NIST ambient particulate matter and diesel engine particles. J Air Waste Manag Assoc 50:1897–1903.

Baulig A, Garlatti M, Bonvallot V, Marchand A, Barouki R, Marano F, et al. 2003. Involvement of reactive oxygen species in the metabolic pathways triggered by diesel exhaust particles in human airway epithelial cells. Am J Physiol Lung Cell Mol Physiol 285:L671–L679.

Beck-Speier I, Dayal N, Karg E, Maier KL, Schumann G, Schulz H, et al. 2005. Oxidative stress and lipid mediators induced in alveolar macrophages by ultrafine particles. Free Radic Biol Med 38:1080–1092.

Bonvallot V, Baeza-Squiban A, Baulig A, Brulant S, Boland S, Muzeau F, et al. 2001. Organic compounds from diesel exhaust particles elicit a proinflammatory response in human airway epithelial cells and induce cytochrome p450 1A1 expression. Am J Respir Cell Mol Biol 25:515–521.

Brunauer S, Emmett PH, Teller E. 1938. Absorption of gases in multimolecular layers. J Am Chem Soc 60:309–319.

Cassinelli ME, O'Connor PF, eds. 1998. NIOSH Method 5040. In: NIOSH Manual of Analytical Methods (NMAM), Second Supplement to NMAM. 4th ed. DHHS (NIOSH) Publication No. 94-113. Cincinnati, OH:National Institute for Occupational Safety and Health. Available: http://www.cdc.gov/niosh/nmam/pdfs/5040.pdf [accessed 2 December 2008].

Castranova V. 2004. Signaling pathways controlling the production of inflammatory mediators in response to crystalline silica exposure: role of reactive oxygen/nitrogen species. Free Radic Biol Med 37:916–925.

Cho HY, Reddy SP, Kleeberger SR. 2006. Nrf2 defends the lung from oxidative stress. Antioxid Redox Signal 8:76–87.

Delfino RJ, Sioutas C, Malik S. 2005. Potential role of ultrafine particles in associations between airborne particle mass and cardiovascular health. Environ Health Perspect 113:934–946.

Dick CA, Brown DM, Donaldson K, Stone V. 2003. The role of free radicals in the toxic and inflammatory effects of four different ultrafine particle types. Inhal Toxicol 15:39–52.

Donaldson K, Tran L, Jimenez LA, Duffin R, Newby DE, Mills N, et al. 2005. Combustion-derived nanoparticles: a review of their toxicology following inhalation exposure. Part Fibre Toxicol 2:10; doi:10.1186/1743-8977-2-10 [Online 21 October 2005].

Duffin R, Clouter A, Brown DM, Tran CL, MacNee W, Stone V, et al. 2002. The importance of surface area and specific reactivity in the acute pulmonary inflammatory response to particles. Ann Occup Hyg 46(suppl 1):242–245.

Frampton MW, Utell MJ, Zareba W, Oberdörster G, Cox C, Huang LS, et al. 2004. Effects of exposure to ultrafine carbon particles in healthy subjects and subjects with asthma. Res Rep Health Eff Inst 126:1–147.

Gharavi N, El-Kadi AO. 2005. Down-regulation of aryl hydrocarbon receptor-regulated genes by tumor necrosis factor-alpha and lipopolysaccharide in murine hepatoma Hepa 1c1c7 cells. J Pharm Sci 94:493–506.

Health Effects Institute. 2002. Understanding the Health Effects of Components of the Particulate Matter Mix: Progress and Next Steps. Health Effects Institute Perspectives Series. Boston, MA:Health Effects Institute.

Heinrich U, Fuhst R, Rittinghausen S, Creutzenberg O, Bellmann B, Koch W, et al. 1995. Chronic inhalation exposure of Wistar rats and 2 different strains of mice to diesel-engine exhaust, carbon-black, and titanium-dioxide. Inhal Toxicol 7:533–556.

Kleeberger SR. 2005. Genetic aspects of pulmonary responses to inhaled pollutants. Exp Toxicol Pathol 57(suppl 1):147–153

Köhle C, Bock KW. 2007. Coordinate regulation of phase I and II xenobiotic metabolisms by the Ah receptor and Nrf2. Biochem Pharmacol 73(12):1853–1862.

Kreyling WG, Semmler M, Moller W. 2004. Dosimetry and toxicology of ultrafine particles. J Aerosol Med 17:140–152.

Li N, Hao M, Phalen RF, Hinds WC, Nel AE. 2003a. Particulate air pollutants and asthma. A paradigm for the role of oxidative stress in PM-induced adverse health effects. Clin Immunol 109:250–265.

Li N, Sioutas C, Cho A, Schmitz D, Misra C, Sempf J, et al. 2003b. Ultrafine particulate pollutants induce oxidative stress and mitochondrial damage. Environ Health Perspect 111:455–460.

Martignoni M, Groothuis GM, de Kanter R. 2006. Species differences between mouse, rat, dog, monkey and human CYP-mediated drug metabolism, inhibition and induction. Expert Opin Drug Metab Toxicol 2:875–894.

Matuschek G, Karg E, Schröppel A, Schulz H, Schmid O. 2007. Chemical investigation of eight different types of carbonaceous particles using thermoanalytical techniques. Environ Sci Technol 41:8406–8411.

Morel Y, Mermod N, Barouki R. 1999. An autoregulatory loop controlling CYP1A1 gene expression: role of H(2)O(2) and NFI. Mol Cell Biol 19:6825–6832.

National Center for Biotechnology Information. 2008. GenBank Overview. Available: http://www.ncbi.nlm.nih.gov/Genbank/ [accessed 25 November 2008].

NIST. 2000. Certificate of Analysis: Standard Reference Material 1650a: Diesel Particulate Matter. National Institute of Standards and Technology. https://srmors.nist.gov/certificates/view_cert2gif.cfm?certificate=1650A [accessed 27 June 2008].

Oberdörster G, Oberdörster E, Oberdörster J. 2005. Nanotoxicology: an emerging discipline evolving from studies of ultrafine particles. Environ Health Perspect 113:823–839.

Piscaglia F, Knittel T, Kobold D, Barnikol-Watanabe S, Di Rocco P, Ramadori G. 1999. Cellular localization of hepatic cytochrome 1B1 expression and its regulation by aromatic hydrocarbons and inflammatory cytokines. Biochem Pharmacol 58:157–165.

Popov I, Lewin G. 1999. Antioxidative homeostasis: characterization by means of chemiluminescent technique. Methods Enzymol 300:437–456.

Rahman I, Yang SR, Biswas SK. 2006. Current concepts of redox signaling in the lungs. Antioxid Redox Signal 8:681–689.

Ramadoss P, Marcus C, Perdew GH. 2005. Role of the aryl hydrocarbon receptor in drug metabolism. Expert Opin Drug Metab Toxicol 1:9–21.

Risom L, Moller P, Loft S. 2005. Oxidative stress-induced DNA damage by particulate air pollution. Mutat Res 592:119–137.

Roth C, Ferron GA, Karg E, Lentner B, Schumann G, Takenaka S, et al. 2004. Generation of ultrafine particles by spark discharging. Aerosol Sci Technol 38:228–235.

Schroeppel A, Lintelmann J, Karg E, Ferron GA. 2003. Physical and chemical characterisation of particles produced by a flame soot aerosol generator (CAST). J Aerosol Sci 34:S1253–S1254.

Sorensen M, Autrup H, Moller P, Hertel O, Jensen SS, Vinzents P, et al. 2003. Linking exposure to environmental pollutants with biological effects. Mutat Res 544:255–271.

Stoeger T, Reinhard C, Takenaka S, Schröppel A, Karg E, Ritter B, et al. 2006. Instillation of six different ultrafine carbon particles indicate a surface area threshold dose for acute lung inflammation in mice. Environ Health Perspect 114:328–333.

Su DS, Jentoft RE, Muller JO, Rothe D, Jacob E, Simpson CD, et al. 2004. Microstructure and oxidation behaviour of Euro IV diesel engine soot: a comparative study with synthetic model soot substances. Catalysis Today 90:127–132.

Takano H, Yanagisawa R, Ichinose T, Sadakane K, Inoue K, Yoshida S, et al. 2002. Lung expression of cytochrome P450 1A1 as a possible biomarker of exposure to diesel exhaust particles. Arch Toxicol 76:146–151.

Till M, Riebniger D, Schmitz HJ, Schrenk D. 1999. Potency of various polycyclic aromatic hydrocarbons as inducers of CYP1A1 in rat hepatocyte cultures. Chem Biol Interact 117:135–150.

Warheit DB, Webb TR, Sayes CM, Colvin VL, Reed KL. 2006. Pulmonary instillation studies with nanoscale TiO2 rods and dots in rats: toxicity is not dependent upon particle size and surface area. Toxicol Sci 91:227–236.

Winyard PG, Moody CJ, Jacob C. 2005. Oxidative activation of antioxidant defence. Trends Biochem Sci 8:453–461.

Wittmaack K. 2007. In search of the most relevant parameter for quantifying lung inflammatory response to nanoparticle exposure: particle number, surface area, or what? Environ Health Perspect 115:187–194.

Xia T, Kovochich M, Brant J, Hotze M, Sempf J, Oberley T, et al. 2006. Comparison of the abilities of ambient and manufactured nanoparticles to induce cellular toxicity according to an oxidative stress paradigm. Nano Lett 6:1794–1807.

Zheng W, Jefcoate CR. 2005. Steroidogenic factor-1 interacts with cAMP response element-binding protein to mediate cAMP stimulation of CYP1B1 via a far upstream enhancer. Mol Pharmacol 67:499–512.